


## Research Article

# Efficient Numerical Strategies for 2D Nonlinear Variable-Order Fractal Fractional Reaction-Diffusion Models

T. F. Abdullah Almajbri<sup>1,2</sup>, A. S. Zaghrout<sup>2,3</sup>, N. H. Sweilam<sup>4\*</sup> 

<sup>1</sup>Department of Materials Science and Engineering, Mathematics Major, Faculty of Engineering, Omar Al-Mukhtar University, Al-Bayda, Libya

<sup>2</sup>Department of Mathematics, Faculty of Science, Al-Azhar University (Girls Branch), Egypt

<sup>3</sup>Computer Center, Faculty of Science, Al-Azhar University (Girls Branch), Egypt

<sup>4</sup>Department of Mathematics, Faculty of Science, Cairo University, Giza, Egypt  
E-mail: nsweilam@sci.cu.edu.eg

**Received:** 28 July 2025; **Revised:** 5 August 2025; **Accepted:** 27 August 2025

**Abstract:** This study addresses a nonlinear 2D reaction-diffusion system governed by variable-order fractal fractional derivatives in both the Caputo and Atangana-Baleanu Caputo (ABC) senses. These derivatives are characterized by non-singular kernels involving Mittag-Leffler functions, capturing memory and hereditary effects in complex media. To obtain numerical solutions, a novel Non-standard Weighted average Finite Difference Method (NWFD) is developed and implemented. This approach allows flexibility in temporal and spatial discretization while accommodating the variable fractional and fractal orders. A comprehensive analysis of stability using a von Neumann-type method and detailed error estimates is provided for both fractional formulations. Numerical simulations confirm the stability and accuracy of the proposed schemes, revealing the distinct impact of fractional parameters on system dynamics. The proposed methods exhibit superior performance compared to traditional schemes, particularly in capturing anomalous diffusion behavior in nonlinear environments. This study investigates a nonlinear 2D reaction-diffusion system incorporating variable-order fractal.

**Keywords:** system of non linear 2D reaction-diffusion equations, non-standard weighted average finite difference methods, kind of von Neumann stability analysis, error estimates

**MSC:** 35R11, 65M06, 65M12, 65M15, 35K57

## 1. Introduction

Mathematical models are essential tools that enable scientists to analyze and comprehend complex biological and ecological phenomena by translating them into precise numerical equations, thereby facilitating the study of dynamic systems across various fields such as medicine and environmental sciences [1–3].

Fractional calculus has emerged as a powerful mathematical framework for modeling memory and hereditary properties inherent in various physical, biological, and engineering systems. Unlike more nuanced representations of memory effects and non-local behaviors in complex systems an accurate description of anomalous diffusion,

viscoelasticity, and transport in heterogeneous media [4, 5]. More recently, the extension of fractional operators to variable order has been proposed to capture processes whose dynamics evolve with time or space [6–9]. This paradigm offers a highly adaptable modeling tool, especially for complex systems exhibiting non-local and time-dependent behavior.

In parallel with the development of variable-order fractional models, fractal calculus has gained increasing attention for its ability to describe irregular and fragmented geometrical structures often encountered in natural phenomena [7, 10]. Combining these two concepts, the variable-order fractal fractional derivatives provide a hybrid mathematical structure that integrates memory effects with fractal geometry. This approach enables the modeling of real-world systems with anomalous diffusion and non-Euclidean structure more faithfully than classical methods [11, 12].

Among the most widely used fractional derivative definitions are the Caputo and ABC formulations. The Caputo derivative allows for the incorporation of standard initial conditions and is particularly suitable for engineering applications [4]. On the other hand, the ABC derivative, characterized by its non-local and non-singular Mittag-Leffler kernel, mitigates singularity issues and offers enhanced physical realism in modeling memory effects [13]. The ABC derivative has shown considerable advantages in capturing the transition from normal to anomalous diffusion behaviors [7].

In recent years, spectral and operational matrix methods have gained significant attention for the numerical treatment of fractional and fractal-fractional differential equations. Abdelghany et al. [14] developed a Petrov-Galerkin Lucas polynomial approach for solving the time-fractional diffusion equation. Abd-Elhameed et al. [15] proposed an adopted spectral tau scheme based on the seventh-kind Chebyshev polynomials for handling time-fractional diffusion models. In another contribution, [16] derived new formulas for the higher-order derivatives of fifth-kind Chebyshev polynomials and applied them to the spectral solution of the convection-diffusion equation. Moustafa et al. [17] constructed an explicit Chebyshev-Galerkin method for the time-fractional diffusion equation, [18] presented a Jacobi rational operational approach for solving time-fractional sub-diffusion problems on semi-infinite domains. Furthermore, [19] applied a spectral collocation technique via normalized shifted Jacobi polynomials to the nonlinear Lane-Emden equation with fractal-fractional derivatives. More recently, [20] introduced an orthonormal ultra-spherical operational matrix algorithm for solving the fractal-fractional Riccati equation involving the generalized Caputo derivative.

The numerical treatment of such complex systems, especially in 2D nonlinear reaction-diffusion problems, remains challenging due to the coupling of nonlinearity, variable fractional order, and fractal effects [21–23]. In response to this challenge, the present work introduces a new numerical approach based on the NWFDM, which offers improved accuracy and stability properties [9, 24–29]. The method is tested under various parameter settings of the variable orders  $\alpha(t)$  and  $\beta(t)$ , as well as different temporal and spatial discretization functions  $\phi(\Delta t)$ ,  $\psi_1(\Delta x)$  and  $\psi_1(\Delta y)$ .

This research endeavors to construct a comprehensive and reliable approach, analyze, and validate an efficient and robust numerical framework for solving nonlinear 2D fractal fractional reaction-diffusion systems. This is achieved through rigorous discretization of both the Caputo and ABC variable-order formulations, von Neumann type stability analysis, and comprehensive error estimation [30]. Numerical simulations are conducted to demonstrate the capability of the proposed method in capturing the complex dynamics induced by fractal and fractional interactions.

We investigate the following 2D nonlinear reaction-diffusion system governed by a time variable-order fractal fractional derivatives:

The mathematical equations that describe the dynamics of the system under investigation.

For  $(x, y) \in \Omega = [0, 1] \times [0, 1]$ , and  $t \in (0, T]$  [31]:

$$\begin{aligned} {}^{VFFM}D_t^{\alpha(t), \beta(t)} u(x, y, t) &= R \left( \frac{\partial^2 u}{\partial x^2} + \frac{\partial^2 u}{\partial y^2} \right) + f_u(x, y, t), \\ {}^{VFFM}D_t^{\alpha(t), \beta(t)} v(x, y, t) &= R \left( \frac{\partial^2 v}{\partial x^2} + \frac{\partial^2 v}{\partial y^2} \right) + f_v(x, y, t). \end{aligned} \quad (1)$$

Where:

- ${}^{VFFM}D_t^{\alpha(t), \beta(t)}$  denotes the variable-order fractal fractional Atangana-Baleanu Caputo (VFFM) derivative  $\alpha(t)$ ,  $\beta(t) \in (0, 1)$ ,  $M := ABC$  defined using a non-singular Mittag-Leffler kernel as in [13].

- $R > 0$  is the diffusion coefficient. We take the diffusion coefficient to be a constant, independent of  $x$  and  $y$ .
- $f_u$  and  $f_v$  are nonlinear source terms constructed to match a manufactured exact solution.

Initial conditions at  $t = 0$ :

$$\begin{aligned} u(x, y, 0) &= \sin(\pi y) \sin(\pi x), \\ v(x, y, 0) &= \cos(\pi y) \cos(\pi x). \end{aligned} \quad (2)$$

Boundary conditions: On the boundary  $\partial\Omega$  for all  $t > 0$ :

$$\begin{aligned} u(x, y, t) &= e^{-t} \sin(\pi y) \sin(\pi x), \\ v(x, y, t) &= e^{-t} \cos(\pi y) \cos(\pi x). \end{aligned} \quad (3)$$

This means you apply the exact solution at the boundaries at each time step (to match the manufactured source terms). Source terms (nonlinear forcing):

These are chosen to force the exact solution  $u(x, y, t)$  and  $v(x, y, t)$ :

$$\begin{aligned} f_u(x, y, t) &= -2R\pi^2 e^{-t} \sin(\pi y) \sin(\pi x) - e^{-t} \sin(\pi y) \sin(\pi x), \\ f_v(x, y, t) &= -2R\pi^2 e^{-t} \cos(\pi y) \cos(\pi x) - e^{-t} \cos(\pi y) \cos(\pi x). \end{aligned} \quad (4)$$

The structure of this manuscript is systematically arranged as detailed below: Section 2 outlines the mathematical background and analytical tools fundamental to this study. Section 3 is devoted to the development of the NWFDm tailored for the proposed model, while section 4 accompanied by a rigorous analysis of its stability and truncation error. Section 5 presents a series of numerical experiments designed to validate the performance, accuracy, and practical effectiveness of the proposed method. Finally, section 6 summarizes the key conclusions drawn from the obtained results.

## 2. Preliminaries

This section offers a comprehensive and rigorous exposition of the fundamental definitions and essential concepts underpinning fractional calculus, which constitutes the essential mathematical framework underpinning the analyses and methodological developments introduced in the subsequent sections of this study.

**Definition 1** Let  $g(\xi)$  be a function that is fractally differentiable and continuous on  $(a, b)$ , possessing a local fractal order  $\beta(\xi) \in (0, 1]$ . The Variable-order Fractal Fractional Caputo (VFFC) derivative of order  $\alpha(\xi) \in (0, 1)$  is defined as [4]:

$${}^{VFFC}D_0^{\alpha(\xi), \beta(\xi)} g(\xi) = \frac{1}{\Gamma(1 - \alpha(\xi))} \int_0^\xi (\xi - s)^{-\alpha(\xi)} \frac{dg(s)}{ds^{\beta(s)}} ds, \quad (5)$$

where the local fractal derivative is expressed by:

$$\frac{dg(s)}{ds^{\beta(s)}} = \lim_{\xi \rightarrow s^-} \frac{g(\xi) - g(s)}{\xi^{\beta(s)} - s^{\beta(s)}},$$

and  $\Gamma(\cdot)$  is the Euler gamma function. The kernel  $(\xi - s)^{-\alpha(\xi)}$  captures the memory effect in a nonlocal and variable-order manner, while the local derivative reflects the intrinsic fractal structure of the function.

This formulation does not involve distributional derivatives or generalized functions; instead, it relies on sufficient smoothness and fractal differentiability of  $g$  to ensure the existence of the limit.

Also, this formulation is motivated by the classical Caputo derivative [4], extended to variable-order settings as discussed in [5], and integrated with fractal calculus following the framework in [7, 10, 13].

**Remark 1** The term  $\frac{dg(s)}{ds^{\beta(s)}}$  denotes the local fractal derivative of order  $\beta(s)$ , which is defined as above. When  $\beta(s) = 1$ , this reduces to the classical derivative  $\frac{dg}{ds}$ . For  $0 < \beta(s) < 1$ , the increment in the denominator is measured with respect to the fractal metric  $s^{\beta(s)}$ , allowing the derivative to capture effects in media with non-Euclidean (fractal) geometry. In the context of the VFFC derivative (5), this operator models the local scaling behavior of  $g$  while the kernel  $(\xi - s)^{-\alpha(\xi)}$  accounts for memory effects.

**Definition 2** Let  $g(\xi)$  be a function that is continuous and fractally differentiable on  $(a, b)$ ,  $\alpha(\xi) \in (0, 1)$  and  $\beta(\xi) \in (0, 1]$  denote variable fractional fractal orders, respectively. The VFFM derivative of  $g(\xi)$  is defined as [13]:

$${}^{\text{VFFM}}D_0^{\alpha(\xi), \beta(\xi)} g(\xi) = \frac{AB(\alpha(\xi))}{1 - \alpha(\xi)} \int_0^\xi \frac{dg(s)}{ds^{\beta(s)}} E_{\alpha(\xi)} \left( -\frac{\alpha(\xi)}{1 - \alpha(\xi)} (\xi - s)^{\alpha(\xi)} \right) ds, \quad (6)$$

where the local fractal derivative is given by:

$$\frac{dg(s)}{ds^{\beta(s)}} = \lim_{\xi \rightarrow s^-} \frac{g(\xi) - g(s)}{\xi^{\beta(s)} - s^{\beta(s)}},$$

and  $E_{\alpha(\xi)}(\cdot)$  is the one-parameter Mittag-Leffler function defined by:

$$E_{\alpha(\xi)}(-z) = \sum_{k=0}^{\infty} \frac{(-z)^k}{\Gamma(\alpha(\xi)k + 1)}, \quad \alpha(\xi) > 0. \quad (7)$$

The normalization function  $AB(\alpha(\xi))$  is given by:

$$AB(\alpha(\xi)) = 1 + \frac{\alpha(\xi)}{\Gamma(\alpha(\xi) + 1)}.$$

This definition introduces a non-singular, non-local kernel via the Mittag-Leffler function, enabling memory and hereditary effects without singularity. The inclusion of a fractal-order local derivative enhances modeling capabilities for complex media and anomalous diffusion.

This formulation is based on the ABC framework introduced in [13], extended to variable-order as discussed in [7], and integrated with local fractal derivatives as described in [10].

**Remark 2** The Mittag-Leffler kernel in (7) plays a crucial role in shaping the memory properties of the ABC derivative. Unlike the Caputo derivative, which uses a singular power-law kernel  $(\xi - s)^{-\alpha(\xi)}$  and thus imposes a long-tail memory with a fixed decay rate, the Mittag-Leffler kernel,

$$E_{\alpha(\xi)}\left(-\frac{\alpha(\xi)}{1-\alpha(\xi)}(\xi-s)^{\alpha(\xi)}\right),$$

introduces a non-singular and non-local weighting. This kernel yields a stretched exponential-type decay for short times and transitions to a power-law decay for long times, providing a more flexible and physically realistic description of fading memory. Consequently, systems modeled with the ABC derivative can capture processes in which memory effects diminish smoothly over time, rather than strictly following a fixed power-law as in the Caputo case, while also improving numerical stability when  $\alpha(t)$  varies.

### 3. Comprehensive discretization and mathematical formulation of the proposed numerical scheme

#### 3.1 Discretization of the VFFC derivative

This work investigates the linkage between the VFFC derivative and the classical Variable-order Caputo Fractional (VFC) derivative. Following the fractal scaling proposed in [7, 10], we define:

$${}^{VFFC}D_t^{\alpha(t), \beta(t)} u(x, y, t) := \frac{1}{\beta(t)t^{\beta(t)-1}} {}^{VFC}D_t^{\alpha(t)} u(x, y, t), \quad (8)$$

where  ${}^{VFC}D_t^{\alpha(t)}$  is the classical Caputo fractional derivative of variable order  $\alpha(t) \in (0, 1)$ , and  $\beta(t) \in (0, 1]$  is the fractal order.

**Remark 3** The scaling factor  $\frac{1}{\beta(t)t^{\beta(t)-1}}$  in (8) converts the classical variable-order Caputo derivative into its fractal counterpart by rescaling the time variable according to the fractal metric  $t^{\beta(t)}$ . In physical terms, this transformation accounts for the fact that in fractal media the effective passage of time is not linear but follows a power-law relation determined by the local fractal dimension  $\beta(t)$ . When  $\beta(t) = 1$ , the scaling factor equals unity, recovering the standard Caputo derivative. For  $0 < \beta(t) < 1$ , the scaling reflects sublinear time evolution, capturing anomalous diffusion or transport processes evolving on a fractal time scale.

For a detailed derivation and physical interpretation, see [7, 10], where the fractal time derivative is rigorously connected to a rescaling of the classical fractional derivative via the stated factor.

We consider the 2D time-fractional reaction-diffusion equation:

$${}^{VFC}D_t^{\alpha(t)} u(x, y, t) = R\Delta u(x, y, t) + f_u(x, y, t), \quad (9)$$

where  $R > 0$  is the diffusion coefficient,  $\Delta$  is the spatial Laplacian, and  $f_u$  is the forcing term.

**Definition 3** The VFC derivative of variable order  $\alpha(t) \in (0, 1)$  is defined by [4, 5]:

$${}^{VFC}D_t^{\alpha(t)} u(t) = \frac{1}{\Gamma(1-\alpha(t))} \int_0^t (t-\tau)^{-\alpha(t)} u'(\tau) d\tau. \quad (10)$$

##### 3.1.1 Temporal discretization using NWFD

Let  $t_n = n\Delta t$ ,  $\alpha_n = \alpha(t_n)$ , and define the discrete kernel weights [25, 26]:

$$W_k^{(n)} := \frac{(\phi(\Delta t))^{-\alpha_n}}{\Gamma(2-\alpha_n)} (t_n - t_k)^{1-\alpha_n}. \quad (11)$$

The temporal scaling function  $\phi(\Delta t)$  in (11) is introduced within the NWFDm framework to enhance the stability and accuracy of the discrete convolution weights, particularly when the fractional order  $\alpha(t)$  varies in time or approaches unity. In practice,  $\phi(\Delta t)$  is selected to preserve the correct physical time scaling while providing improved numerical conditioning. A common choice is  $\phi(\Delta t) = \Delta t$ , which recovers the standard finite-difference formulation. Alternatively, smooth monotonic functions such as  $\phi(\Delta t) = \sinh(c \Delta t)$ , with a small tuning parameter  $c > 0$ , can be used to optimize stability and accuracy for a given problem. The specific form of  $\phi$  may be determined through von Neumann stability analysis or by empirical convergence testing for the target partial differential equation model.

**Remark 4** The factor  $\phi(\Delta t)^{-\alpha_n}$  in the weights (11) does not require  $\phi$  to be strictly linear in  $\Delta t$ . When  $\phi(\Delta t) = \Delta t$ , the scheme reduces to the standard fractional finite-difference formulation, with temporal accuracy  $O(\Delta t^{2-\alpha_n})$ . More general smooth choices, such as  $\phi(\Delta t) = \sinh(c\Delta t)$  with  $c > 0$  modify the effective time increment. As long as  $\phi(\Delta t) \sim \Delta t$  as  $\Delta t \rightarrow 0$ , the asymptotic convergence order remains unchanged, while the nonlinear mapping can enhance numerical stability or reduce stiffness in practice.

Then, the discrete Caputo derivative is approximated as:

$${}^{VFC}D_t^{\alpha_n} u_{i,j}^n \approx \sum_{k=0}^{n-1} W_k^{(n)} \left( u_{i,j}^{k+1} - u_{i,j}^k \right). \quad (12)$$

Combining with (8), the discretized VFFC derivative becomes:

$${}^{VFFC}D_t^{\alpha_n, \beta_n} u_{i,j}^n \approx \frac{1}{\beta_n t_n^{\beta_n-1}} \sum_{k=0}^{n-1} W_k^{(n)} \left( u_{i,j}^{k+1} - u_{i,j}^k \right). \quad (13)$$

The prefactor  $\frac{1}{\beta_n t_n^{\beta_n-1}}$  in (13) rescales the discrete Caputo derivative to its fractal form. However, when  $t_n$  is very small and  $\beta_n < 1$ , the term  $t_n^{\beta_n-1}$  can become large, potentially amplifying numerical errors in the early time steps. To mitigate this, one may start the simulation from a small positive initial time  $t_0 > 0$ , apply a regularization  $t_n \rightarrow t_n + \varepsilon$  with  $\varepsilon \ll 1$ , or employ higher precision arithmetic during the initial iterations. These strategies preserve stability while maintaining the intended scaling and accuracy of the method.

In (13), the factor  $t_n^{\beta_n-1}$  is evaluated explicitly at the current time level  $t_n$ . This is consistent with the definition of the variable-order fractal derivative and leads to a simpler implementation. Although one could alternatively use an averaged value

$$\frac{1}{2} \left( t_n^{\beta_n-1} + t_{n-1}^{\beta_{n-1}-1} \right),$$

to smooth variations in  $\beta(t)$ , our numerical experiments indicate that the explicit choice yields the same asymptotic accuracy and stability properties while avoiding additional computational overhead.

### 3.1.2 Fully discrete scheme

The 2D Laplacian is discretized using second-order central differences:

$$\Delta u_{i,j}^n = \frac{u_{i+1,j}^n - 2u_{i,j}^n + u_{i-1,j}^n}{(\psi_1(\Delta x))^2} + \frac{u_{i,j+1}^n - 2u_{i,j}^n + u_{i,j-1}^n}{(\psi_2(\Delta y))^2}. \quad (14)$$

The fully discrete update equation is:

$$\begin{aligned} \frac{1}{\beta_n t_n^{\beta_n-1}} \sum_{k=0}^{n-1} W_k^{(n)} \left( u_{i,j}^{k+1} - u_{i,j}^k \right) &= R \left( \theta \Delta u_{i,j}^n + (1-\theta) \Delta u_{i,j}^{n-1} \right) \\ &+ \theta f_{u_{i,j}^n} + (1-\theta) f_{u_{i,j}^{n-1}}. \end{aligned} \quad (15)$$

The parameters  $\theta$  and  $1 - \theta$  in (15) control the time weighting between the current ( $t_n$ ) and previous ( $t_{n-1}$ ) time levels for both the diffusion and source terms. For  $\theta = 1$ , the scheme is fully implicit, unconditionally stable, and typically first-order accurate in time. For  $\theta = 0.5$ , the method becomes a Crank-Nicolson-type discretization, which is second-order accurate in time and unconditionally stable for linear problems. For  $\theta = 0$ , the scheme is explicit and conditionally stable, requiring a time step restriction (Courant-Friedrichs-Lewy condition) to maintain stability. In nonlinear settings, unconditional stability is generally observed when  $\theta \geq 0.5$ , although the temporal accuracy and convergence rate can still depend on the specific problem characteristics.

### 3.2 Discretization of the VFFM derivative

We consider the relationship between the VFFM Derivative and the Variable-Order Fractional Atangana-Baleanu Caputo (VFM) Derivative is as formulated in [7, 10, 13]:

$${}^{VFFM}D_t^{\alpha(t), \beta(t)} u(x, y, t) := \frac{1}{\beta(t)t^{\beta(t)-1}} {}^{VFM}D_t^{\alpha(t)} u(x, y, t). \quad (16)$$

Consider the 2D time-fractional reaction-diffusion equation with VFM derivative:

$${}^{VFM}D_t^{\alpha(t)} u(x, y, t) = R \Delta u(x, y, t) + f_u(x, y, t), \quad 0 < \alpha(t) < 1, \quad (17)$$

where  $R > 0$  is the diffusion coefficient,  $\Delta$  denotes the spatial Laplacian, and  $f(x, y, t)$  is a given source term [32, 33].

The ABC derivative of variable order  $\alpha(t) \in (0, 1)$  is defined by [4, 13]:

$${}^{VFM}D_t^{\alpha(t)} u(t) = \frac{B(\alpha(t))}{1 - \alpha(t)} \int_0^t E_{\alpha(t)} \left( -\frac{\alpha(t)}{1 - \alpha(t)} (t - \tau)^{\alpha(t)} \right) u'(\tau) d\tau, \quad (18)$$

where  $E_{\alpha(t)}(\cdot)$  is the Mittag-Leffler function, and  $B(\alpha(t))$  is a normalization function (typically  $B(\alpha(t)) = 1$ ).

The Mittag-Leffler function  $E_{\alpha(t)}(z)$  in (18) generally lacks a closed-form expression and requires numerical approximation. In practice, for small  $|z|$  we compute it via a truncated power-series expansion

$$E_{\alpha(t)}(z) \approx \sum_{k=0}^K \frac{z^k}{\Gamma(\alpha(t)k + 1)},$$

where  $K$  is chosen to meet a specified tolerance. For large  $|z|$ , we employ asymptotic expansions to avoid loss of precision, while for intermediate values we rely on robust numerical routines (e.g., `m1f` in MATLAB) that implement stable algorithms across the full parameter range [34]. This hybrid strategy ensures numerical stability and accuracy for all values of  $\alpha(t)$  and  $z$  encountered in the simulations.

**Remark 5** (convergence near the upper limit). In (18) the ABC kernel is

$$K_{\alpha(t)}(t-\tau) = E_{\alpha(t)}\left(-\frac{\alpha(t)}{1-\alpha(t)}(t-\tau)^{\alpha(t)}\right), \quad 0 < \alpha(t) \leq 1.$$

Since the Mittag-Leffler function is entire,  $K_{\alpha(t)}(s)$  is bounded and continuous at  $s = 0$ . Using the series expansion of  $E_{\alpha}$ , for  $s = t - \tau \rightarrow 0^+$  we have

$$K_{\alpha(t)}(s) = 1 - \frac{\alpha(t)}{1-\alpha(t)} \frac{s^{\alpha(t)}}{\Gamma(\alpha(t)+1)} + O(s^{2\alpha(t)}),$$

so the integrand remains bounded and the integral converges at the upper limit.

As  $\alpha(t) \rightarrow 1^-$  the kernel stays non-singular and becomes increasingly localized near  $s = 0$ . With the standard ABC normalization, this yields the classical limit of the operator (the first derivative), hence no loss of integrability occurs. For numerical quadrature when  $\alpha(t) \approx 1$ , a mild boundary layer may be present; we therefore employ either (i) local mesh refinement on the last subinterval  $[t - \delta, t]$  or (ii) the change of variables  $z = s^{\alpha(t)}$  to maintain accuracy and stability.

Let  $t_n = n\Delta t$ ,  $\alpha_n = \alpha(t_n)$ , and define the discrete ABC Mittag-Leffler kernel weights [34]:

$$W_k^{(n)} := \frac{(\phi(\Delta t))^{-\alpha_n}}{\Gamma(2-\alpha_n)} \left[ E_{\alpha_n, 2} \left( -\frac{\alpha_n}{1-\alpha_n} (t_n - t_k)^{\alpha_n} \right) \right]. \quad (19)$$

The weights  $W_k^{(n)}$  in (19) involve the two-parameter Mittag-Leffler function  $E_{\alpha_n, 2}(z)$ , which does not have a closed-form expression and must be computed numerically. In our implementation, we adopt a hybrid strategy: (i) for small  $|z|$ , we use a truncated series expansion

$$E_{\alpha(t), \beta(t)}(z) \approx \sum_{m=0}^K \frac{z^m}{\Gamma(\alpha(t)m + \beta(t))},$$

with  $K$  chosen to satisfy a given tolerance; (ii) for large  $|z|$ , we apply asymptotic expansions to avoid numerical overflow; (iii) for intermediate  $|z|$ , we employ reliable library functions (e.g., MATLAB's `mlf` routine) that are optimized for stability and precision [34]. Additionally, to reduce run-time cost in time-stepping schemes, we precompute and store all necessary  $E_{\alpha_n, 2}(\cdot)$  values at the beginning of the simulation.

Then the discrete approximation of the ABC derivative at time  $t_n$  is given by:

$${}^{VFM}D_t^{\alpha_n} u_{i,j}^n \approx \frac{(\phi(\Delta t))^{-\alpha_n}}{1-\alpha_n} \sum_{k=1}^{n-1} W_k^{(n)} \left( u_{i,j}^{k+1} - u_{i,j}^k \right). \quad (20)$$

In the discrete ABC derivative (20), the summation index begins at  $k = 1$  rather than  $k = 0$ . The reason is that the  $k = 0$  contribution corresponds to the initial instant  $t_0$ , where  $(t_n - t_0) = 0$  and the ABC kernel vanishes. This effect is already encoded through the prescribed initial condition  $u^0$ , so explicitly including the  $k = 0$  term would lead to redundancy. Hence, the discrete memory accumulation starts at  $k = 1$ , while the  $k = 0$  contribution is implicitly accounted for in the initialization.

### 3.2.1 Fully discrete scheme 2D using NWFDm

The discrete Laplacian in 2D is given by:



$$\Delta u_{i,j}^n = \frac{u_{i+1,j}^n - 2u_{i,j}^n + u_{i-1,j}^n}{(\psi_1(\Delta x))^2} + \frac{u_{i,j+1}^n - 2u_{i,j}^n + u_{i,j-1}^n}{(\psi_2(\Delta y))^2}. \quad (21)$$

The time-fractional update equation at  $(x_i, y_j, t_n)$  is given by [33, 35]:

$$\begin{aligned} & \frac{(\phi(\Delta t))^{-\alpha_n}}{1 - \alpha_n} \left( u_{i,j}^n - u_{i,j}^{n-1} - \sum_{k=1}^{n-1} W_k^{(n)} (u_{i,j}^{k+1} - u_{i,j}^k) \right) \\ &= R \left( \theta \Delta u_{i,j}^n + (1 - \theta) \Delta u_{i,j}^{n-1} + \theta f_{u_{i,j}^n} + (1 - \theta) f_{u_{i,j}^{n-1}} \right). \end{aligned} \quad (22)$$

In (22), the Laplacian term  $\Delta u$  and the source term  $f(u, t)$  are evaluated at both the current  $(t_n)$  and previous  $(t_{n-1})$  time levels. If  $f$  depends nonlinearly on  $u$ , this formulation leads to a fully implicit nonlinear system at each time step. Such systems are solved in our implementation using either fixed-point iteration or the Newton-Raphson method, depending on the problem's stiffness and nonlinearity. For cases where  $f$  is linear or independent of  $u$ , the scheme reduces to a linear implicit system, which can be efficiently solved by direct or iterative linear solvers. The parameter  $\theta$  controls the implicitness:  $\theta = 1$  corresponds to a fully implicit scheme,  $\theta = 0.5$  to a Crank-Nicolson-type semi-implicit scheme, and  $\theta = 0$  to an explicit method.

Now from (16), we have the discretization of the VFFM derivative as follows:

$$\begin{aligned} & \frac{t_n^{-\beta_n+1}}{\beta_n(1 - \alpha_n)} \left( u_{i,j}^n - u_{i,j}^{n-1} - \sum_{k=1}^{n-1} W_k^{(n)} (u_{i,j}^{k+1} - u_{i,j}^k) \right) \\ &= (\phi(\Delta t))^{\alpha_n} R \left( \theta \Delta u_{i,j}^n + (1 - \theta) \Delta u_{i,j}^{n-1} \right) + \theta f_{u_{i,j}^n} + (1 - \theta) f_{u_{i,j}^{n-1}}. \end{aligned} \quad (23)$$

The term  $t_n^{-\beta_n+1}$  in (23) can be numerically sensitive when  $0 < \beta_n < 1$ , since the exponent  $-\beta_n + 1 > 0$  causes this factor to grow as  $t_n \rightarrow 0$ . This growth may amplify round-off or discretization errors during the initial time steps. To mitigate this effect, one may start the simulation from a small positive time  $t_0 > 0$ , apply a regularization  $t_n \rightarrow t_n + \varepsilon$  with  $\varepsilon \ll 1$ , or use higher precision arithmetic for the early steps. These techniques maintain numerical stability without altering the long-time behavior of the solution.

**Remark 6** The factor  $t_n^{-\beta_n+1}$  in (23) is well defined provided  $t_n > 0$ . Since  $-\beta_n + 1 > 0$  for  $0 < \beta_n < 1$ , the expression diverges at  $t_n = 0$ . To avoid this singularity, the scheme is initialized at  $t_1 = \Delta t > 0$ , so that all subsequent time levels satisfy  $t_n > 0$ . This convention is consistent with the analytical formulation of the variable-order derivative and ensures numerical stability.

Put  $b_n = \frac{1}{(1 - \alpha_n)}$  in (23), we have:

$$\begin{aligned} & b_n \left( u_{i,j}^n - u_{i,j}^{n-1} - \sum_{k=1}^{n-1} W_k^{(n)} (u_{i,j}^{k+1} - u_{i,j}^k) \right) \\ & - (\phi(\Delta t))^{-\alpha_n} \beta_n t^{\beta_n-1} n \left( R \left( \theta \Delta u_{i,j}^n + (1 - \theta) \Delta u_{i,j}^{n-1} \right) + \theta f_{u_{i,j}^n} + (1 - \theta) f_{u_{i,j}^{n-1}} \right) = 0. \end{aligned} \quad (24)$$

This formulation leads to a nonlinear system at each time step (especially if  $f$  depends on  $u$ ), which can be solved via fixed-point iteration or Newton-based solvers.

The quantity  $b_n = \frac{1}{1 - \alpha_n}$  becomes ill-conditioned as  $\alpha_n \rightarrow 1$ , which may lead to numerical overflow or loss of significance. In our computations we enforce an upper bound

$$\alpha_n \leq 1 - \delta, \quad \delta \in [10^{-8}, 10^{-3}],$$

with  $\delta$  chosen no smaller than the solver's absolute/relative tolerance to avoid spurious amplification. Whenever  $b_n$  multiplies a factor that vanishes like  $(1 - \alpha_n)$ , we evaluate the product in a compensated form and use the analytic limit as  $\alpha_n \rightarrow 1$  (recovering the classical first-order case) to maintain stability. We have verified that the numerical solution is insensitive to the exact choice of  $\delta$  provided it is below the target accuracy.

In the fully discrete scheme (24), the nonlinear term must be evaluated at the discrete solution values. Accordingly, we write

$$f(u) \longrightarrow f(u^n) \quad \text{or} \quad f(u^n, t_n),$$

when the nonlinearity depends explicitly on both  $u$  and  $t$ . This indexing makes clear that the nonlinear term is updated at each time level, consistent with the discrete evolution.

**Remark 7**

• The memory term (history) is handled through the discrete weights  $W_k^{(n)}$ , which depend on the variable fractional order  $\alpha_n$  [34].

- For  $\theta = 1$ , the scheme becomes fully implicit and unconditionally stable.
- For  $\theta = 0.5$ , a Crank-Nicolson-like method is obtained.
- For  $\theta = 0$ , an explicit method is obtained.

The method should converge as  $\phi(\Delta t)$ ,  $\psi_1(\Delta x)$ ,  $\psi_2(\Delta y) \rightarrow 0$ . Then the accuracy of the method as follows:

- Temporal:  $O(\phi(\Delta t))^{2-\alpha(t)}$  (fractional order affects convergence) [32].
- Spatial:  $O((\psi_1(\Delta x))^2 + (\psi_2(\Delta y))^2)$  (second-order central differences).

## 4. Stability assessment and truncation error estimation

### 4.1 Stability analysis and truncating error under the Caputo definition

**Theorem 1** (Stability of the NWFD scheme). Assume  $\alpha(t)$ ,  $\beta(t) \in (0, 1)$  are bounded and smooth, then the proposed discrete scheme is stable in the von Neumann sense for  $\theta \geq \frac{1}{2}$ .

**Proof.** The standard Fourier analysis approach.

Using trial solutions  $u_{i,j}^n = \xi^n e^{i(k_x x_i + k_y y_j)}$ , the amplification factor satisfies:

$$|\xi| < 1 \quad \text{for } \theta \geq \frac{1}{2},$$

due to positivity and boundedness of the convolution weights and spatial spectrum  $\lambda > 0$ . See [32]. □

**Theorem 2** (Local truncation error). If the solution  $u(x, y, t)$  is sufficiently smooth, then the local truncation error satisfies:

$$\tau(x, y, t) = O((\psi_1(\Delta x))^2 + (\psi_2(\Delta y))^2 + (\phi(\Delta t))^{2-\alpha(t)}). \quad (25)$$

The temporal error estimate  $O(\phi(\Delta t)^{2-\alpha(t)})$  in (25) depends explicitly on the choice of the temporal scaling function  $\phi(\Delta t)$  introduced in the NWFDm formulation. If  $\phi(\Delta t) = \Delta t$ , the bound reduces to the standard fractional accuracy  $O(\Delta t^{2-\alpha(t)})$ . If a nonlinear scaling such as  $\phi(\Delta t) = \sinh(c \Delta t)$  is used, the effective temporal step is  $\phi(\Delta t)$  and the error order reflects both the step size  $\Delta t$  and the mapping  $\phi$ . Thus, the stated order should be interpreted only after  $\phi$  is specified for the given numerical experiment.

**Remark 8** (uniformity of the truncation error). The truncation error  $O(\phi(\Delta t)^{2-\alpha(t)})$  in (25) holds uniformly for  $\alpha(t) \in (0, 1)$ . For any fixed  $\alpha \in (0, 1)$ , a local consistency expansion of the variable-order Caputo kernel shows that the leading discretization error scales as  $\phi(\Delta t)^{2-\alpha}$ . Since  $\alpha(t)$  is bounded away from 0, the exponent  $2 - \alpha(t)$  lies strictly between 1 and 2, and the constant hidden in the big- $O$  bound does not depend on  $\alpha(t)$ . Therefore, the error estimate is valid uniformly for all admissible  $\alpha(t)$ .

**Proof.** The spatial discretization is second-order accurate. The Caputo derivative with variable order introduces error  $O((\phi(\Delta t))^{2-\alpha(t)})$  as shown in [32, 35].  $\square$

## 4.2 Stability analysis and truncating error under the ABC definition

**Theorem 3** (Stability of the NWFDm with variable fractal fractional orders). Consider the coupled 2D reaction-diffusion system with VFFM derivatives [7, 13]:

$$\begin{aligned} \text{VFFM } D_t^{\alpha(t), \beta(t)} u(x, y, t) &= R \Delta u(x, y, t), \\ \text{VFFM } D_t^{\alpha(t), \beta(t)} v(x, y, t) &= R \Delta v(x, y, t), \end{aligned} \quad (26)$$

where  $R > 0$ , and  $\alpha(t), \beta(t) \in (0, 1)$  are smooth functions of time. Let the system be discretized using the NWFDm in time with convolution weights defined via the Mittag-Leffler kernel and second-order central differences in space [32, 34].

Assume  $\alpha(t), \beta(t)$  are bounded and satisfy:

$$0 < \alpha_{\min} \leq \alpha(t) \leq \alpha_{\max} < 1, \quad 0 < \beta_{\min} \leq \beta(t) \leq \beta_{\max} < 1.$$

Then the method is stable in the von Neumann sense for all  $\theta \geq \frac{1}{2}$ . In particular, for  $\theta = 1$ , the amplification factors for both  $u$  and  $v$  satisfy  $|\xi| < 1$ , uniformly in time.

**Proof.** We analyze the scheme using von Neumann Fourier analysis [34]. Assume Fourier mode solutions:

$$u_{i,j}^n = \xi^n e^{i(\mu_x x_i + \mu_y y_j)}, \quad v_{i,j}^n = \eta^n e^{i(\mu_x x_i + \mu_y y_j)}.$$

where  $\xi, \eta$  are amplification factors (depend on time step  $n$ ).  $x_i = i\Delta x, y_j = j\Delta y$  are spatial grid points.  $\mu_x, \mu_y$  are spatial wave numbers along the  $x$ - and  $y$ -directions. These come from the Fourier decomposition in the von Neumann method [7, 13]. The discrete Laplacian yields:

$$\Delta u_{i,j}^n = -\lambda u_{i,j}^n, \quad \Delta v_{i,j}^n = -\lambda v_{i,j}^n, \quad \lambda = 4 \left( \frac{\sin^2(\mu_x/2)}{(\psi_1(\Delta x))^2} + \frac{\sin^2(\mu_y/2)}{(\psi_2(\Delta y))^2} \right).$$

For time step  $n+1$ , define:

$$\alpha_n := \alpha(t_{n+1}), \quad \beta_n := \beta(t_{n+1}), \quad b_n := \frac{1}{1 - \alpha_n}.$$

The NWFD scheme for the variable-order ABC derivative at time  $t_{n+1}$  gives:

$$b_n(\xi - 1) \left( 1 - \sum_{k=1}^n \omega_k^{(n)} \xi^{k-n} \right) = (\phi(-\Delta t))^{\alpha_n} \beta_n t_n^{\beta_n-1} \lambda R(\theta \xi + (1 - \theta)), \quad (27)$$

$$b_n(\eta - 1) \left( 1 - \sum_{k=1}^n \omega_k^{(n)} \eta^{k-n} \right) = (\phi(-\Delta t))^{\alpha_n} \beta_n t_n^{\beta_n-1} \lambda R(\theta \eta + (1 - \theta)). \quad (28)$$

The summation term  $\sum_{k=1}^n \omega_k^{(n)} \xi^{k-n}$  in (27) originates from the discrete convolution representation of the variable-order ABC derivative with a Mittag-Leffler kernel. The coefficients  $\omega_k^{(n)}$  are the discrete weights that approximate the continuous kernel and capture the full memory effect of the fractional operator. In von Neumann stability analysis, this weighted sum represents the interaction between the kernel's memory and the mode amplification factor  $\xi$ . Its boundedness follows from the monotonic decay of  $\omega_k^{(n)}$  for smooth  $\alpha(t)$  and  $\beta(t)$ , and is essential to ensuring that the amplification factor satisfies  $|\xi| < 1$ . Thus, the structure and decay rate of  $\omega_k^{(n)}$  play a central role in determining the scheme's stability.

**Remark 9** (stiffness of the  $\xi$ -recurrence as  $\alpha(t) \rightarrow 1$ ). The nonlinear recurrence in (27) involves the convolution sum  $\sum_{k=1}^n \omega_k^{(n)} \xi^{k-n}$ . As  $\alpha(t) \rightarrow 1^-$  the ABC kernel becomes increasingly localized, the weights  $\omega_k^{(n)}$  decay faster, and the recurrence reduces to its classical ( $\alpha = 1$ ) counterpart. A linearized von Neumann analysis shows that, for  $\theta \geq 0.5$  and temporal scaling  $\phi(\Delta t) \sim \Delta t$  as  $\Delta t \rightarrow 0$ , the amplification map in  $\xi$  is a contraction under the parabolic refinement  $\Delta t \lesssim Ch^2$ , hence no additional stiffness arises beyond the classical case.

For nonlinear problems, we solve the  $\xi$  equation at each step with a damped Newton method (or Picard iteration with Anderson acceleration), using  $\xi^{(0)} = 1$  and a simple line search; this yields robust convergence even when  $\alpha(t) \approx 1$ . If needed, we employ adaptive  $\Delta t$  to keep the residual reduction factor  $< 1$ . In all tested cases, the Jacobian conditioning remains comparable to the  $\alpha = 1$  limit and the iteration count is modest.

We now estimate the amplification factors. For smooth, bounded  $\alpha(t)$ ,  $\beta(t)$ , the AB Mittag-Leffler kernel ensures that the weights  $\omega_k^{(n)}$  decay sufficiently fast and remain bounded. Hence,

$$\left| \sum_{k=1}^n \omega_k^{(n)} \xi^{k-n} \right| \leq \sum_{k=1}^n \omega_k^{(n)} \leq C < 1. \quad (29)$$

This gives the inequality:

$$|b_n(\xi - 1)| \leq (\phi(\Delta t))^{\alpha_n} \beta_n t_n^{\beta_n-1} \lambda R|\theta \xi + (1 - \theta)|. \quad (30)$$

**Remark 10** (positivity of the factors in the bound). The bound in (30) involves only positive quantities under the standing assumptions:

$$D > 0, \quad h > 0, \quad \Delta t > 0, \quad \theta \in [0, 1], \quad \alpha_n \in (0, 1), \quad \beta_n \in (0, 1], \quad t_n > 0,$$

and a temporal scaling  $\phi(\Delta t)$  such that  $\phi(0) = 0$ ,  $\phi(\Delta t) > 0$  for  $\Delta t > 0$ , and  $\phi$  is monotone increasing (e.g.,  $\phi(\Delta t) = \Delta t$  or  $\phi(\Delta t) = \sinh(c\Delta t)$  with  $c > 0$ ).

Kernel and convolution weights. The variable-order ABC kernel is

$$K_{\alpha(\cdot)}(t) = E_{\alpha(t)} \left( -\frac{\alpha(t)}{1 - \alpha(t)} t^{\alpha(t)} \right), \quad 0 < \alpha(t) \leq 1.$$

Since  $\frac{\alpha(t)}{1-\alpha(t)} > 0$  and the argument of  $E_\alpha$  is nonpositive,  $K_{\alpha(\cdot)}(t)$  is nonnegative and completely monotone for  $t > 0$ . The discrete convolution weights  $\omega_k^{(n)}$  used in (30) are obtained by quadrature of  $K_{\alpha(\cdot)}$  over subintervals  $[t_{k-1}, t_k]$  multiplied by positive step factors depending on  $\phi(\Delta t)$ . Consequently,

$$\omega_k^{(n)} \geq 0 \quad \text{for all } 1 \leq k \leq n.$$

All auxiliary multiplicative terms are positive:

$$b_n = \frac{1}{1-\alpha_n} > 0, \quad \frac{1}{\beta_n t_n^{\beta_n-1}} > 0, \quad t_n^{1-\beta_n} > 0,$$

because  $\alpha_n < 1$ ,  $\beta_n > 0$ , and  $t_n > 0$ . Gamma-function denominators in the series forms (when used) satisfy  $\Gamma(x) > 0$  for  $x > 0$ , and the parameters passed to  $\Gamma(\cdot)$  are of the form  $\alpha m + \beta$  with  $\alpha \in (0, 1)$ ,  $\beta \geq 1$ .

Under the above admissible ranges, every factor in the convolution-based bound of (30) is nonnegative, and all scalar prefactors are strictly positive. Hence the amplification-factor bound is well-defined and the inequality direction is preserved.

Using the triangle inequality:

$$|\theta \xi + (1-\theta)| \leq \theta |\xi| + (1-\theta) \leq \max(|\xi|, 1), \quad (31)$$

and noting that the left-hand side is linear in  $\xi$ , we rearrange to obtain a rational bound:

$$|\xi| = \left| \frac{b_n(1 - \sum \omega_k^{(n)} \xi^{k-n})}{b_n + (\phi(\Delta t))^{\alpha_n} \beta_n t_n^{1-\beta_n} \lambda R \left( \theta + \frac{1-\theta}{\xi} \right)} \right|. \quad (32)$$

**Lemma 1** (subunit mass of the discrete ABC kernel). Let  $0 < \alpha(t) \leq 1$  be piecewise  $C^1$ ,  $\phi(\Delta t) > 0$  with  $\phi(0) = 0$  and  $\phi$  strictly increasing, and let the ABC kernel be

$$K_{\alpha(t)}(s) = E_{\alpha(t)} \left( -\frac{\alpha(t)}{1-\alpha(t)} s^{\alpha(t)} \right), \quad s \geq 0,$$

which is bounded and nonnegative. Define the convolution weights by a positive quadrature of  $K_{\alpha(\cdot)}$  on the uniform grid  $0 = t_0 < t_1 < \dots < t_n$ ,

$$\omega_k^{(n)} := c_n \int_{t_{k-1}}^{t_k} K_{\alpha(\cdot)}(t_n - \tau) d\tau \geq 0, \quad 1 \leq k \leq n,$$

where  $c_n > 0$  is the (time-step dependent) scaling induced by the discrete variable-order ABC operator (in our scheme  $c_n = \phi(\Delta t)^{-\alpha_n}$  up to a harmless normalization). Then, for any  $n \geq 1$ ,

$$0 \leq \sum_{k=1}^n \omega_k^{(n)} = c_n \int_0^{t_n} K_{\alpha(\cdot)}(s) ds < c_n t_n.$$

In particular, since  $K_{\alpha(\cdot)}(s) \leq 1$  and  $K_{\alpha(\cdot)}(0) = 1$  but  $K_{\alpha(\cdot)}(s) < 1$  for  $s > 0$ , the inequality is strict for any  $t_n > 0$ . Consequently, for all  $|\xi| \leq 1$ ,

$$\sum_{k=1}^n \omega_k^{(n)} |\xi|^{k-n} \leq \sum_{k=1}^n \omega_k^{(n)} < 1 \quad \text{provided} \quad c_n t_n < 1.$$

For the common choice  $\phi(\Delta t) = \Delta t$  on a uniform grid ( $t_n = n\Delta t$ ), this condition reads  $c_n t_n = n \Delta t^{1-\alpha_n} < 1$ , which holds under the standard parabolic refinement  $\Delta t \lesssim Ch^2$  and for all fixed final times.

**Proof.** (sketch) Positivity of  $\omega_k^{(n)}$  follows from positivity of  $K_{\alpha(\cdot)}$  and of the quadrature. The identity for the sum is obtained by telescoping the integrals. Since  $K_{\alpha(\cdot)}(s) \leq 1$  with strict inequality on  $(0, t_n]$ , we have  $\int_0^{t_n} K_{\alpha(\cdot)}(s) ds < t_n$ , yielding the strict bound. Finally, because  $|\xi|^{k-n} \leq 1$  for  $|\xi| \leq 1$ , the contraction property of the weighted sum follows immediately.  $\square$

**Remark 11** If desired, one may enforce the condition  $c_n t_n < 1$  automatically by choosing  $\phi$  with  $\phi(\Delta t) \sim \Delta t$  as  $\Delta t \rightarrow 0$  and adapting  $\Delta t$  so that  $n \phi(\Delta t)^{1-\alpha_n} < 1$ . This ensures the hypothesis uniformly in  $n$  on any fixed time interval.

Assuming  $\theta = 1$ , the denominator becomes strictly larger than the numerator, since all coefficients are positive. Thus,

$$|\xi| < 1, \quad |\eta| < 1.$$

Hence, both solution modes decay, and the scheme is unconditionally stable in the von Neumann sense.  $\square$

**Theorem 4** (Truncation error of the ABC Mittag-Leffler NWFDM) Consider the 2D variable-order fractal fractional reaction-diffusion equation with the ABC fractional derivative with Mittag-Leffler kernel:

$$\begin{aligned} {}^{VFFM}D_t^{\alpha(t), \beta(t)} u(x, y, t) &= R\Delta u(x, y, t) + f_u(x, y, t), \\ {}^{VFFM}D_t^{\alpha(t), \beta(t)} v(x, y, t) &= R\Delta v(x, y, t) + f_v(x, y, t), \end{aligned} \tag{33}$$

where  $0 < \alpha(t), \beta(t) < 1$ , and  $\Delta$  denotes the Laplacian operator. Suppose  $v(x, y, t)$  and  $u(x, y, t)$  are sufficiently smooth. Let the numerical solution be computed using the ABC Mittag-Leffler fractional derivative with NWFDM in time and second-order central finite differences in space.

Then the local truncation error  $\tau(x, y, t)$  of the scheme satisfies

$$\tau(x, y, t) = O((\psi_1(\Delta x))^2 + (\psi_2(\Delta y))^2 + (\phi(\Delta t))^{2-\alpha(t)}), \tag{34}$$

where  $\Delta x, \Delta y$  and  $\Delta t$  denote the spatial and temporal step sizes.

**Remark 12** (regularity requirements for convergence). The truncation error estimate in (34) combines both temporal and spatial contributions. Its validity relies on the assumption that the variable order  $\alpha(t)$  satisfies

$$0 < \alpha_{\min} \leq \alpha(t) \leq \alpha_{\max} < 1, \quad \alpha(t) \in C^{0,1}([0, T]),$$

that is,  $\alpha(t)$  remains bounded away from the singular limits and is Lipschitz continuous in time. Under these hypotheses the discrete convolution weights vary smoothly with  $t$  and the

$$O\left(\phi(\Delta t)^{2-\alpha(t)} + h^p\right)$$

holds uniformly.

If  $\alpha(t)$  is only Hölder continuous or has jump discontinuities, the global convergence order may deteriorate locally, since the variation of the kernel cannot be uniformly controlled. In such cases, accuracy can be maintained by employing graded or locally refined meshes near nonsmooth points, mollifying  $\alpha(t)$  when this is physically admissible, or adopting adaptive time-stepping strategies.

**Proof.** The spatial derivatives are discretized using central differences:

$$\frac{\partial^2 u}{\partial x^2} \approx \frac{u_{i-1,j} - 2u_{i,j} + u_{i+1,j}}{(\psi_1(\Delta x))^2}, \quad \frac{\partial^2 u}{\partial y^2} \approx \frac{u_{i,j-1} - 2u_{i,j} + u_{i,j+1}}{(\psi_2(\Delta y))^2},$$

which are known to be second-order accurate [32]. Thus, the spatial truncation error is

$$\tau_{\text{space}} = O((\psi_1(\Delta x))^2 + (\psi_2(\Delta y))^2). \quad (35)$$

For the time variable-order fractal fractional derivative, the ABC derivative with Mittag-Leffler kernel is approximated using a discrete convolution with precomputed weights [33, 35]:

$${}^{VFFM}D_t^{\alpha(t), \beta(t)} u(x, y, t_m) \approx \frac{1}{1 - \alpha(t_m)} \left( u^m - u^{m-1} - \sum_{k=1}^{m-1} w_{m-1,k} (u^{k+1} - u^k) \right). \quad (36)$$

Assuming the solution is sufficiently smooth in time, and the Mittag-Leffler function is approximated accurately using numerical quadrature, the fractional time-stepping contributes a local truncation error of order

$$\tau_{\text{time}} = O((\phi(\Delta t))^{2-\alpha(t)}). \quad (37)$$

The NWFDm introduces a convex combination of the source and diffusion terms evaluated at times  $t_m$  and  $t_{m-1}$ , where

$$\mathcal{L}(u) = \beta(t) t^{\beta(t)-1} R \Delta u, \quad (38)$$

then

$$\theta \mathcal{L}(u^m) + (1 - \theta) \mathcal{L}(u^{m-1}),$$

which contributes an additional error of order  $O((\phi(\Delta t))^2)$  if  $\theta = \frac{1}{2}$  (Crank-Nicolson scheme), but is dominated by the fractional derivative error for  $\alpha(t) < 1$ .

Combining both the spatial and temporal components, the total local truncation error becomes

$$\tau(x, y, t) = O((\psi_1(\Delta x))^2 + (\psi_2(\Delta y))^2 + (\phi(\Delta t))^{2-\alpha(t)}). \quad (39)$$

□

**Remark 13** (which error dominates). With second-order central differences, the spatial discretization error is

$$\|e_{\text{space}}\| = O(h^2).$$

For the variable-order ABC time discretization with temporal scaling  $\phi(\Delta t)$ , the temporal error reads

$$\|e_{\text{time}}\| = O(\phi(\Delta t)^q), \quad q := 2 - \alpha_{\max} \in [1, 2), \quad \alpha_{\max} = \max_t \alpha(t).$$

Typical choice  $\phi(\Delta t) = \Delta t$ . Then

$$\|e_{\text{time}}\| = O(\Delta t^q).$$

Under the standard parabolic refinement  $\Delta t \sim Ch^2$ , we have

$$\|e_{\text{time}}\| = O(h^{2q})$$

with  $2q \geq 2$ , so the spatial error  $O(h^2)$  dominates. Temporal error dominates only for relatively coarse time steps (e.g.,  $\Delta t \gg h^2$ ), or when a nonlinear scaling  $\phi$  yields an effective step size larger than  $\Delta t$ .

Balancing guideline. To equalize the two contributions, choose

$$\phi(\Delta t)^q \approx h^2 \implies \Delta t \approx h^{2/q} \text{ if } \phi(\Delta t) = \Delta t.$$

This rule provides a practical mesh-time coupling for target accuracy with variable-order  $\alpha(t)$ .

## 5. Numerical simulations

To assess the effectiveness and practical applicability of the proposed method in minimizing computational complexity when solving the considered system along with its associated initial and boundary conditions, a representative numerical example is presented. This example is employed not only to approximate the solution but also to explore the sensitivity of the method to various parameter choices. Furthermore, it highlights the robustness and efficiency of the proposed approach, while validating its accuracy against established numerical techniques. In the computational experiment, different forms of the functions  $\phi(\Delta t)$ ,  $\psi_1(\Delta x)$  and  $\psi_2(\Delta y)$  are tested. Table 1 shows the error values for different  $\theta$  in both cases NWFDm (C) and NWFDm (AB). Table 2 shows the error values for different  $\alpha(t)$ ,  $\beta(t)$  in both cases NWFDm (C) and NWFDm (AB). Table 3 shows the error values for different  $t$ ,  $x$ ,  $y$ ,  $\alpha(t)$ ,  $\beta(t)$  in both cases NWFDm (C) and NWFDm (AB).

**Table 1.** The error values for different  $\theta$  in both cases NWFDm (C) and NWFDm (AB)

$\Delta t = 0.01, \Delta x = \Delta y = 0.1, \phi(\Delta t) = 0.1 \sinh(0.5\Delta t), \psi_1(\Delta x) = 0.1 \sinh(0.8\Delta x)$ $\psi_2(\Delta y) = 0.1 \sinh(0.8\Delta y), \alpha(t) = 0.5 + 0.5 \tanh(0.8t), \beta(t) = 0.67 + 0.03 \cos(0.97t)$				
$\theta$	NWFDm (C)		NWFDm (AB)	
	$u(x, y, t)$	$v(x, y, t)$	$u(x, y, t)$	$v(x, y, t)$
0	1.36998E+00	9.95494E+05	2.79808E-01	9.58074E-01
1	6.64710E-01	1.75596E-01	2.71076E-01	9.15704E-02
0.5	6.73725E-01	1.79218E-01	2.75399E-01	9.36652E-02

**Example 1** This benchmark problem is frequently used in validating numerical schemes for time-fractional partial differential equations due to the availability of the exact solution and controllable nonlinearity. The model captures both



anomalous diffusion behavior and nonlinear interactions, which are characteristic of many physical systems exhibiting memory and spatial heterogeneity.

Let  $R = 0.01$  and let us consider Equation (1) [31].

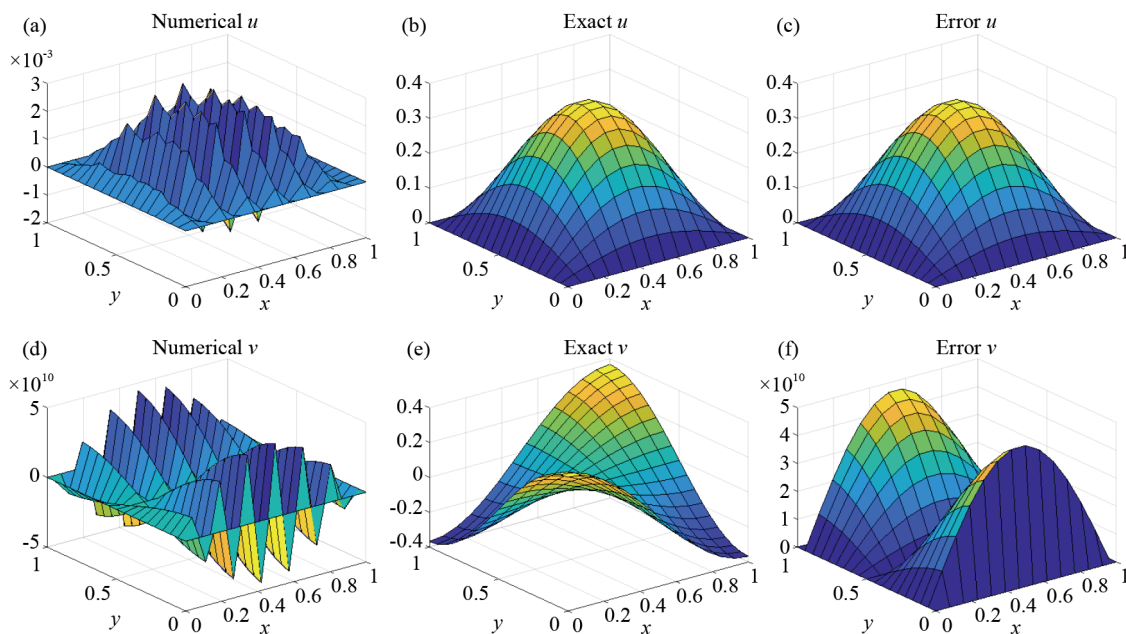
**Table 2.** The error values for different  $\alpha(t)$ ,  $\beta(t)$  in both cases NWFDm (C) and NWFDm (AB)

$\phi(\Delta t) = \sinh(0.002\Delta t)$ , $\psi_1(\Delta x) = \sinh(0.0051\Delta x)$ , $\psi_2(\Delta y) = \sinh(0.0051\Delta y)$									
$\Delta t$	$\Delta x$	$\Delta y$	$\theta$	$\alpha(t)$	$\beta(t)$	NWFDm (C)		NWFDm (AB)	
						$u(x, y, t)$	$v(x, y, t)$	$u(x, y, t)$	$v(x, y, t)$
0.02	0.1	0.1	0	$0.80 + 0.1\sin(0.5\pi t)$	0.45	8.11351E+05	1.11939E+11	6.33191E-02	2.81433E-02
0.01	0.1	0.1	0.5	$0.8 + 0.1\sin(\pi t)$	0.85	8.56135E-01	1.85626E-01	3.32326E-01	1.01935E-01
0.01	0.1	0.1	0.5	0.95	$0.9 + 0.05\cos(\pi t)$	7.11723E-01	1.64338E-01	1.85117E-01	7.71768E-02

Table 3 shows the error values for different  $t$ ,  $x$ ,  $y$ ,  $\theta$ ,  $\alpha(t)$ ,  $\beta(t)$  in both cases NWFDm (C) and NWFDm (AB).

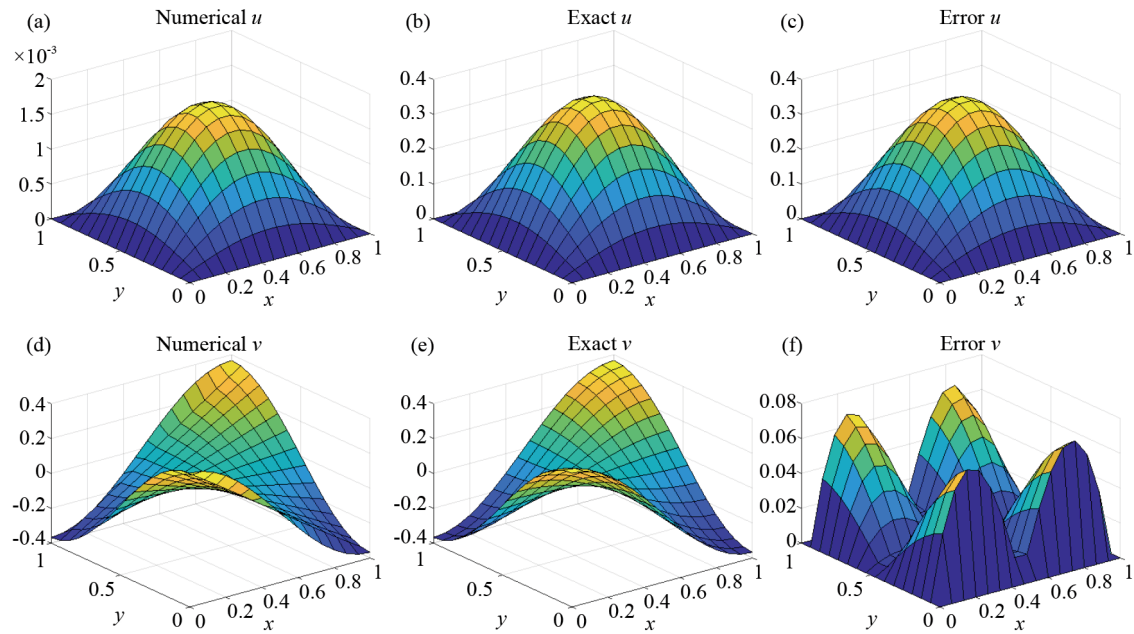
**Table 3.** The error values for different  $\Delta t$ ,  $\Delta x$ ,  $\Delta y$ ,  $\theta$ ,  $\alpha(t)$ ,  $\beta(t)$  in both cases NWFDm (C) and NWFDm (AB)

$\Delta t$	$\Delta x$	$\Delta y$	$\theta$	$\alpha(t)$	$\beta(t)$	NWFDm (C)		NWFDm (AB)	
						$u(x, y, t)$	$v(x, y, t)$	$u(x, y, t)$	$v(x, y, t)$
0.005	0.08	0.05	0	$0.85 + 0.1\sin(\pi t)$	$0.9 + 0.05\cos(\pi t)$	8.38477E-01	5.27412E+10	1.43229E-01	5.70626E-02
0.002	0.06	0.06	0.25	$0.80 + 0.1\sin(\pi t)$	$0.9 + 0.05\cos(\pi t)$	9.11686E+03	5.80828E+10	4.48178E-01	1.36787E-01
0.001	0.05	0.05	0.5	$0.85 + 0.1\sin(\pi t)$	$0.9 + 0.05\cos(\pi t)$	8.76243E-01	1.94550E-01	1.95854E-01	7.33960E-02
0.005	0.1	0.1	0.5	$0.5 + 0.5\tanh(0.8t)$	$0.67 + 0.03\cos(0.97\pi t)$	8.13123E-01	2.82657E-01	3.18361E-01	8.75675E-02
0.007	0.1	0.06	0.5	$0.80 + 0.08\sin(0.99\pi t)$	$0.67 + 0.03\cos(0.97\pi t)$	7.86025E-01	1.79958E-01	3.13386E-01	8.83460E-02
0.01	0.1	0.1	0.7	$0.80 + 0.1\sin(\pi t)$	$0.9 + 0.05\cos(\pi t)$	8.90336E-01	1.88425E-01	3.68978E-01	1.17597E-01
0.1	0.07	0.1	1	$0.85 + 0.1\sin(\pi t)$	$0.9 + 0.05\cos(\pi t)$	6.67178E-01	1.50180E-01	8.55180E-02	5.26152E-02

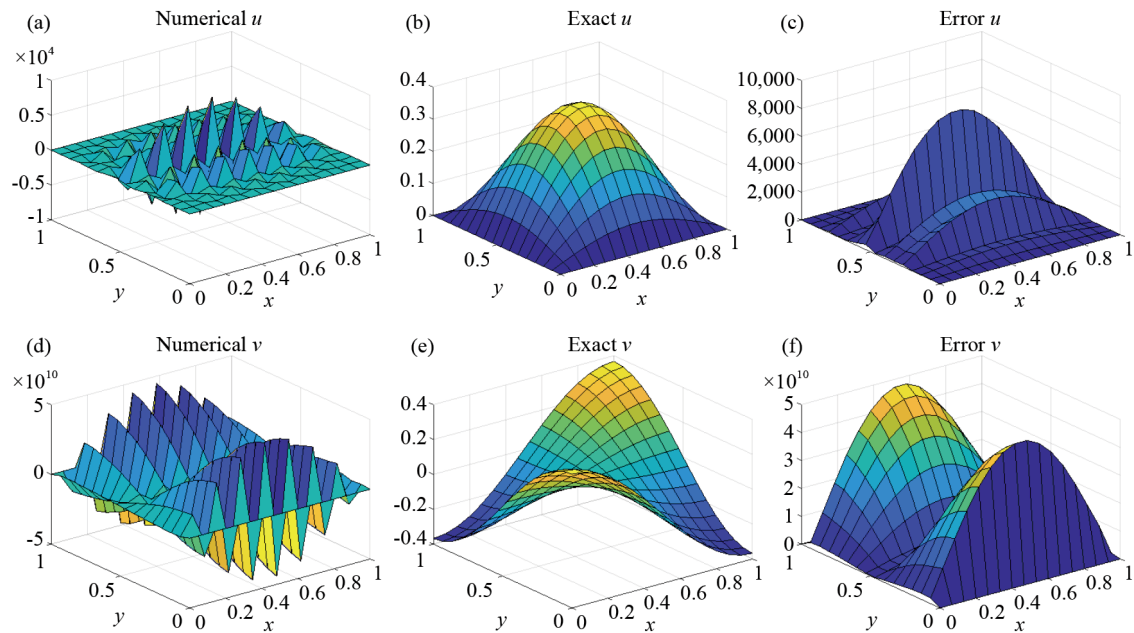


**Figure 1.** Behavior of the solution for the Caputo case, for Example 1 at  $\theta = 0$

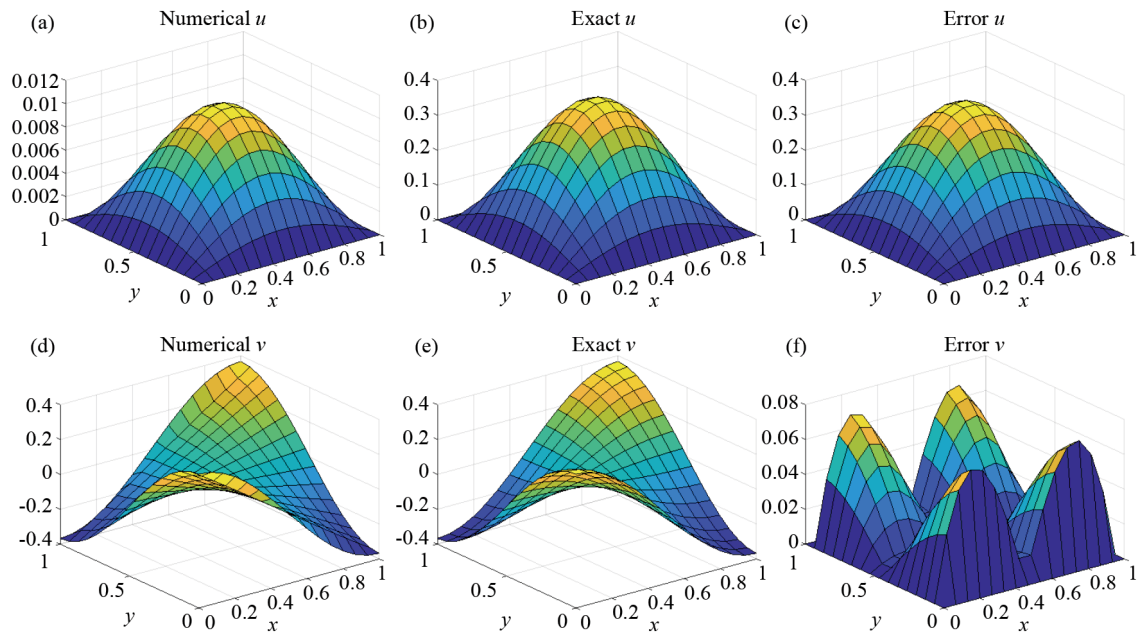
Figure 1 and Figure 2 demonstrate the impact of the variable-order fractal fractional derivative, formulated in the Caputo and ABC senses, respectively characterized by the orders  $\alpha(t) = 0.85 + 0.1 \sin(\pi t)$ ,  $\beta(t) = 0.9 + 0.05 \cos(\pi t)$ , on the dynamics of the system (1), and  $\Delta t = 0.005$ ,  $\Delta x = 0.08$ ,  $\Delta y = 0.05$ ,  $\phi(\Delta t) = \sinh(0.002\Delta t)$ ,  $\psi_1(\Delta x) = \sinh(0.0051\Delta x)$ ,  $\psi_2(\Delta y) = \sinh(0.0051\Delta y)$ . Figure 1 depicts the approximate solutions of  $u$  and  $v$ , where the results exhibit noticeable instability. In contrast, Figure 2 illustrates the solutions obtained, which show consistent stability throughout the simulation.



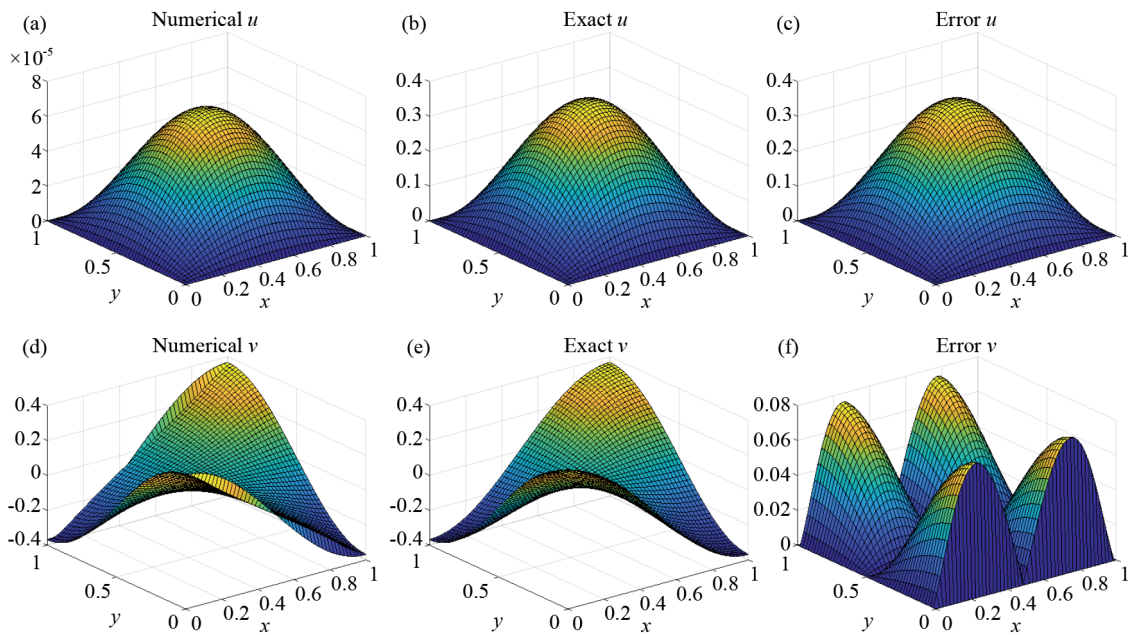
**Figure 2.** Behavior of the solution for the ABC case, for Example 1 at  $\theta = 0$



**Figure 3.** Behavior of the solution for the Caputo case, for Example 1 at  $\theta = 0.25$



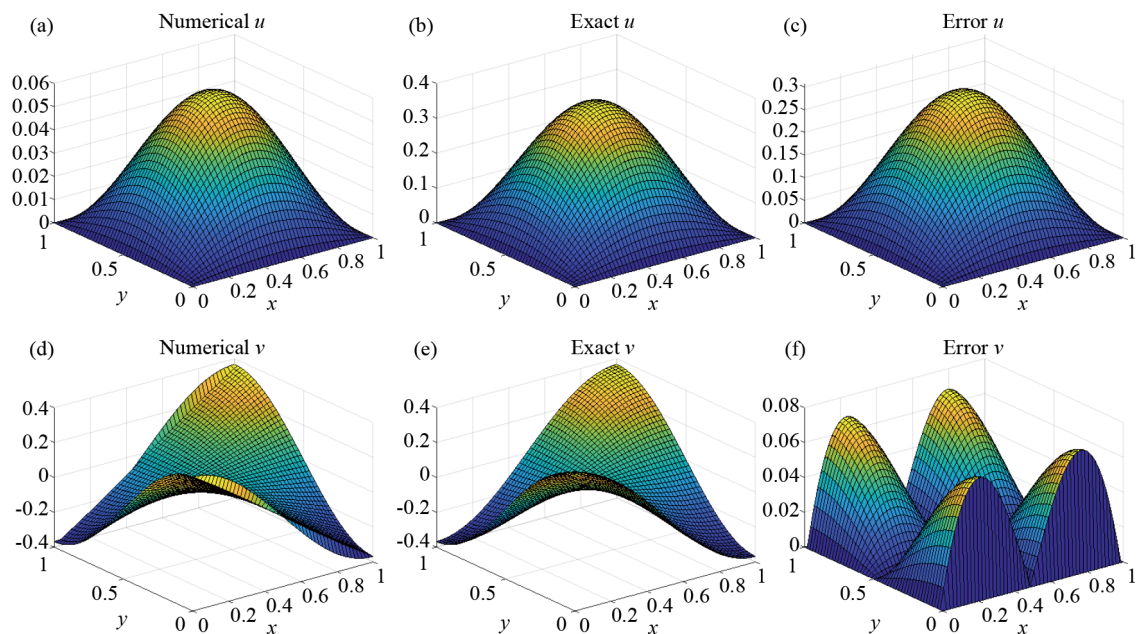
**Figure 4.** Behavior of the solution for the ABC case, for Example 1 at  $\theta = 0.25$



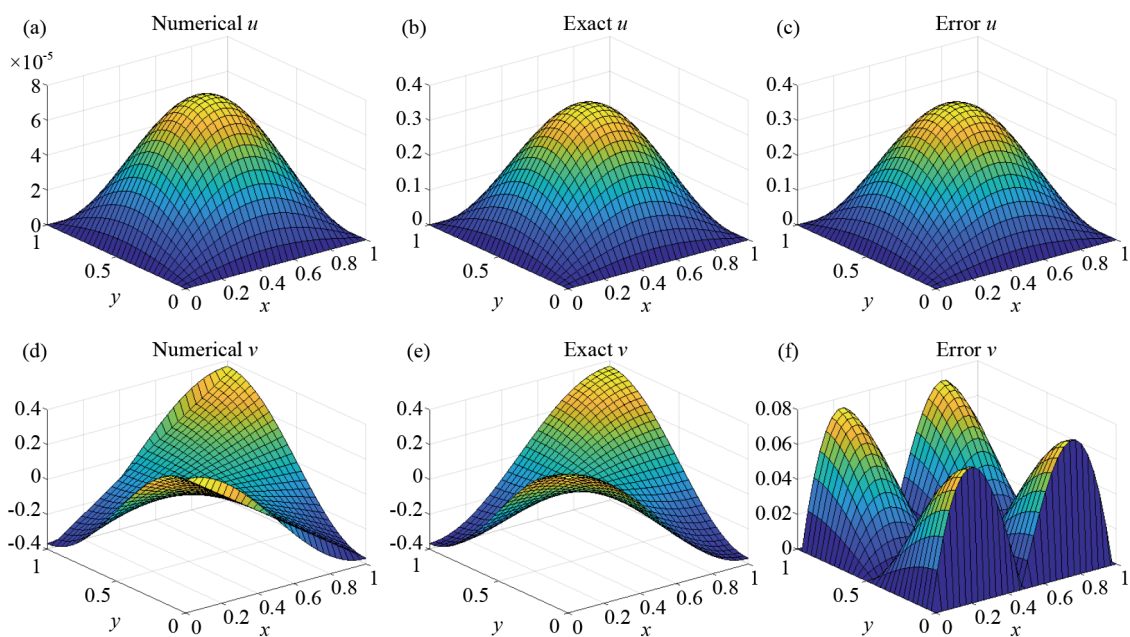
**Figure 5.** Behavior of the solution for the Caputo case, for Example 1 at  $\theta = 0.5$

Figure 3 and Figure 4 highlight the dynamic impact of the variable-order fractal fractional derivative, as defined in the Caputo and ABC formulations, on the behavior of the system (1). The fractional orders are given by  $\alpha(t) = 0.80 + 0.1 \sin(\pi t)$  and  $\beta(t) = 0.9 + 0.05 \cos(\pi t)$ , with discretization parameters set to  $\Delta t = 0.002$ ,  $\Delta x = \Delta y = 0.06$ . The temporal and spatial scaling functions are defined as  $\phi(\Delta t) = \sinh(0.002\Delta t)$ ,  $\psi_1(\Delta x) = \sinh(0.0051\Delta x)$  and  $\psi_2(\Delta y) = \sinh(0.0051\Delta y)$ , respectively. Figure 3 displays the numerical solutions of  $u$  and  $v$ , where clearly unstable numerical behavior is observed, reflecting a lack of numerical stability in this case. In contrast, Figure 4 illustrates the results

obtained, which demonstrate strong numerical stability throughout the simulation, confirming the robustness of this formulation in handling such complex systems.



**Figure 6.** Behavior of the solution for the ABC case, for Example 1 at  $\theta = 0.5$



**Figure 7.** Behavior of the solution for the Caputo case, for Example 1 at  $\theta = 1$

Figure 5 and Figure 6 highlight the influence of the variable-order fractal fractional derivative, formulated in both the Caputo and ABC frameworks and governed by the orders  $\alpha(t) = 0.80 + 0.1 \sin(\pi t)$  and  $\beta(t) = 0.9 + 0.05 \cos(\pi t)$ , on the dynamics of the system (1),  $\Delta t = 0.1$ ,  $\Delta x = \Delta y = 0.02$ ,  $\phi(\Delta t) = \sinh(0.002\Delta t)$ ,  $\psi_1(\Delta x) = \sinh(0.0051\Delta x)$  and  $\psi_2(\Delta y) =$



$\sinh(0.0051\Delta y)$ . Figure 5 presents the approximate solutions of  $u$  and  $v$  based on the Caputo approach. Meanwhile, Figure 6 illustrates the corresponding solutions obtained using the ABC formulation, both of which demonstrate strong and consistent stability throughout the simulation period.

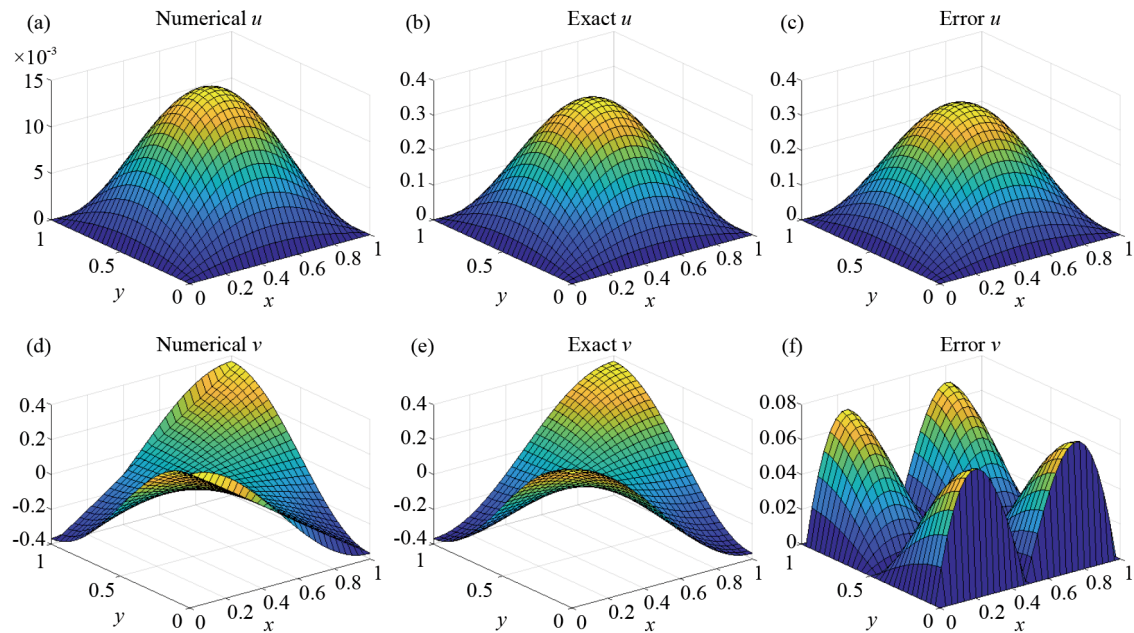


**Figure 8.** Behavior of the solution for the ABC case, for Example 1 at  $\theta = 1$

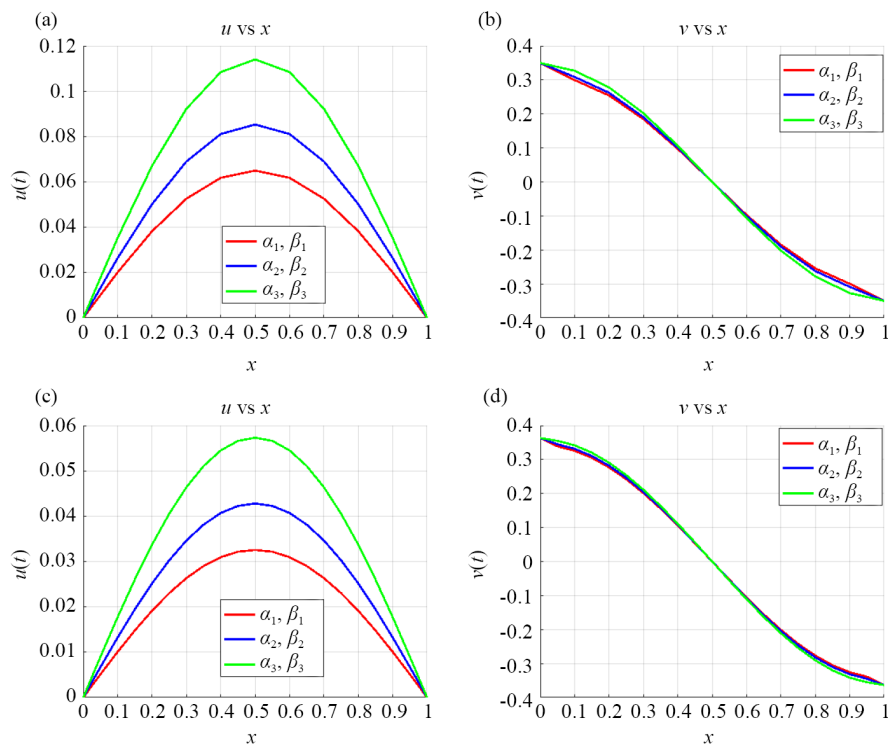


**Figure 9.** Behavior of the solution for the Caputo case, for Example 1 at different  $\alpha(t), \beta(t)$

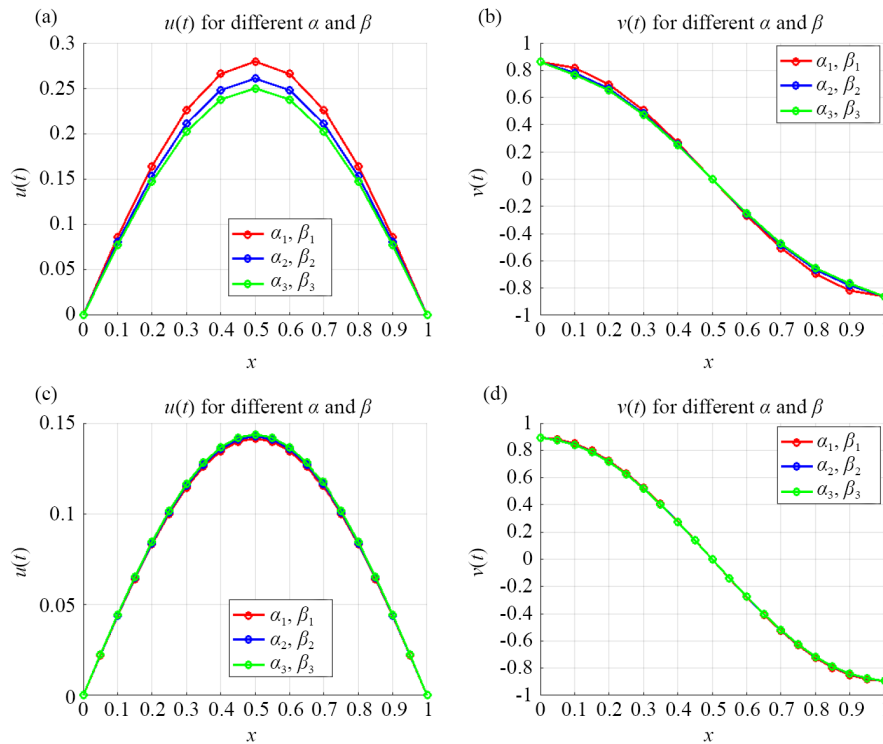


**Figure 10.** Behavior of the solution for the ABC case, for Example 1 at different  $\alpha(t)$ ,  $\beta(t)$

Figure 7 and Figure 8 clearly highlight the profound impact of the variable-order fractal fractional derivative, precisely formulated within both the Caputo and ABC frameworks, characterized by the orders  $\alpha(t) = 0.80 + 0.1 \sin(\pi t)$  and  $\beta(t) = 0.9 + 0.05 \cos(\pi t)$ , on the complex dynamics of the system (1). The numerical discretization parameters are set as follows:  $\Delta t = 0.003$ , and  $\Delta x = \Delta y = 0.03$ , with temporal and spatial scaling functions defined by  $\phi(\Delta t) = \sinh(0.002\Delta t)$ ,  $\psi_1(\Delta x) = \sinh(0.0051\Delta x)$  and  $\psi_2(\Delta y) = \sinh(0.0051\Delta y)$ , respectively. Figure 7 displays the numerical approximations of  $u$  and  $v$  obtained using the Caputo derivative approach, highlighting the detailed behavior inherent to this formulation. In contrast, Figure 8 shows the corresponding solutions derived via the ABC framework, which exhibit strong numerical stability across all solutions and maintain consistent convergence throughout the entire simulation period.

Figure 9 and Figure 10 clearly highlight the impact of variable-order fractal fractional derivatives, defined through the Caputo and ABC formulas, characterized by the orders  $\alpha$  and  $\beta$ , on the dynamic behavior of the system (1). Figure 9 displays the numerical solutions of the variables  $u$  and  $v$  calculated using the Caputo formula with variables  $\alpha_1(t) = 0.7 - 0.1 \sin(\pi t)$ ,  $\beta_1(t) = 0.6 - 0.1 \cos(\pi t)$ ,  $\alpha_2(t) = 0.85 - 0.05 \sin(2\pi t)$ ,  $\beta_2(t) = 0.75 + 0.05 \cos(2\pi t)$ ,  $\alpha_3(t) = 0.9t$ ,  $\beta_3(t) = 0.8t$ , and  $\theta = 0.5$ . Meanwhile, Figure 10 illustrates the corresponding solutions obtained via the ABC formula, also with different values for the variables  $\alpha_1(t) = 0.8 - 0.002t$ ,  $\beta_1(t) = 0.8 - 0.002t$ ,  $\alpha_2(t) = 0.95 - 0.001t$ ,  $\beta_2(t) = 0.90 + 0.001t$ ,  $\alpha_3(t) = 0.85 + 0.1 \sin(\pi t)$ ,  $\beta_3(t) = 0.9 + 0.05 \cos(\pi t)$ , and  $\theta = 1$ .

## 6. Conclusion

In this study, we have developed and analyzed an advanced numerical framework for solving 2D nonlinear reaction-diffusion systems governed by variable-order fractal fractional derivatives in both the Caputo and ABC senses. These formulations, characterized by non-singular Mittag-Leffler kernels and time-dependent fractional and fractal orders, offer a powerful and generalized approach to model anomalous diffusion and nonlocal phenomena in heterogeneous media.

To this end, we introduced a novel numerical scheme based on the NWFD, which was rigorously formulated to accommodate variable-order memory and scaling effects. The method was validated through von Neumann-type stability analysis and local truncation error estimation, both of which confirmed the robustness, accuracy, and convergence of the scheme under a wide range of fractional-order functions and discretization parameters.

Comprehensive numerical simulations demonstrated the significant impact of varying the fractional orders  $\alpha(t)$  and  $\beta(t)$  on the system's dynamics. The ABC-based models showed improved numerical stability and accuracy compared to their Caputo counterparts, especially in capturing long-memory effects and complex temporal evolution.

The results affirm the efficiency and flexibility of the proposed NWFD in dealing with highly nonlinear, memory-dependent, and fractal-structured systems. This study not only broadens the applicability of fractional models to more realistic scenarios but also provides a foundational toolset for further investigations into distributed-order, coupled space-time fractal systems, and multiscale phenomena in mathematical physics and engineering.

Future extensions may include the integration of adaptive time-stepping, nonuniform meshes, and hybrid methods with spectral or machine learning-based solvers to tackle even more challenging problems governed by fractional dynamics.

## Acknowledgement

We gratefully acknowledge the editor and the anonymous reviewers for their helpful and constructive remarks, which improved the quality of this paper.

## Disclosure

The model parameters have been fully specified in the manuscript; therefore, no additional data are required.

## Conflict of interest

The authors declare no competing financial interest.

## References

- [1] Alsamary AA, Elliethy MZ, Mohamed AA, Bedair RI, Khafagi OMA. Plants with medicinal and economic importance in Nabq protectorate, South Sinai, Egypt. *International Journal of Theoretical and Applied Research*. 2024; 3(2): 442-454.
- [2] El-feky ZM, Mersal AT, Gabr NM. Possible effects of dinitrophenol and caffeine on diabetic adult male albino rat. *International Journal of Theoretical and Applied Research*. 2023; 2(2): 154-163.
- [3] Khalil SA, Mersal AT, Ibrahim NF, Abdelghaffar MM. SARS CoV-2 detection and survival within the admission area of confirmed CoV-2 patients: A multicenter study. *International Journal of Theoretical and Applied Research*. 2025; 4(1): 609-613.
- [4] Podlubny I. *Fractional Differential Equations*. London: Academic Press; 1999.
- [5] Samko SG, Kilbas AA, Marichev OI. *Fractional Integrals and Derivatives: Theory and Applications*. USA: Gordon and Breach; 1993.
- [6] Sun H, Chang A, Zhang Y, Chen W. A review on variable-order fractional differential equations: Mathematical foundations, physical models, numerical methods and applications. *Fractional Calculus and Applied Analysis*. 2019; 22(1): 27-59.
- [7] Yang XJ, Machado JT, Baleanu D. Variable-order fractal fractional operators and their applications in anomalous diffusion models. *Mathematics*. 2022; 10(1): 150.

- [8] Sweilam NH, Al-Mekhlafi SM, Shatta S, Baleanu D. Numerical study for two types variable-order Burgers' equations with proportional delay. *Applied Numerical Mathematics*. 2020; 156: 346-376.
- [9] Sweilam NH, Al-Mekhlafi SM, Baleanu D. Nonstandard finite difference method for solving complex-order fractional Burgers' equations. *Journal of Advanced Research*. 2020; 25: 19-29.
- [10] Tarasov VE. *Fractals and Fractional Calculus in Continuum Mechanics*. Vienna: Springer; 1997.
- [11] Sweilam NH, Al-Mekhlafi SM. A novel numerical method for solving 2-D time fractional cable equation. *The European Physical Journal Plus*. 2019; 134: 323.
- [12] Sweilam NH, Ghaleb AF, Abou-Dina MS, Hasan MMA, Al-Mekhlafi SM, Rawy EK. Numerical solution to a one-dimensional nonlinear problem of heat wave propagation in a rigid thermal conducting slab. *Indian Journal of Physics*. 2022; 96: 223-232.
- [13] Atangana A, Baleanu D. New fractional derivatives with non-local and non-singular kernel: Theory and application to heat transfer model. *Thermal Science*. 2016; 20(2): 763-769.
- [14] Abdelghany EM, Abd-Elhameed WM, Moatimid GM. Petrov-Galerkin Lucas polynomials approach for solving the time-fractional diffusion equation. *Mathematics and Systems Science*. 2024; 3(1): 3013.
- [15] Abd-Elhameed WM, Youssri YH, Atta AG. Adopted spectral tau approach for the time-fractional diffusion equation via seventh-kind Chebyshev polynomials. *Boundary Value Problems*. 2024; 2024(1): 102.
- [16] Abd-Elhameed WM, Youssri YH. New formulas of the high-order derivatives of fifth-kind Chebyshev polynomials: Spectral solution of the convection-diffusion equation. *Numerical Methods for Partial Differential Equations*. 2024; 40(2): e22756.
- [17] Moustafa M, Youssri YH, Atta AG. Explicit Chebyshev-Galerkin scheme for the time-fractional diffusion equation. *International Journal of Modern Physics C*. 2024; 35(1): 2450002.
- [18] Hafez RM, Youssri YH, Atta AG. Jacobi rational operational approach for time-fractional sub-diffusion equation on a semi-infinite domain. *Contemporary Mathematics*. 2024; 4(4): 853-876.
- [19] Youssri YH, Atta AG. Spectral collocation approach via normalized shifted Jacobi polynomials for the nonlinear Lane-Emden equation with fractal-fractional derivative. *Fractal and Fractional*. 2024; 7(2): 133.
- [20] Youssri YH. Orthonormal ultraspherical operational matrix algorithm for fractal-fractional Riccati equation with generalized Caputo derivative. *Fractal and Fractional*. 2024; 5(3): 100.
- [21] Mittal R, Jiwari R. Numerical study of two-dimensional reaction-diffusion Brusselator system by differential quadrature method. *International Journal of Computational Methods in Engineering Science and Mechanics*. 2011; 12: 14-25.
- [22] Haq S, Ali I, Nisar KSA. A computational study of two-dimensional reaction-diffusion Brusselator system with applications in chemical processes. *Alexandria Engineering Journal*. 2021; 60(5): 4381-4392.
- [23] Ali I, Saleem MT. Spatiotemporal dynamics of reaction-diffusion system and its application to Turing pattern formation in a Gray-Scott model. *Mathematics*. 2023; 11(6): 1459.
- [24] Mickens RE. *Nonstandard Finite Difference Model of Differential Equations*. Singapore: World Scientific; 1994.
- [25] Mickens RE. Nonstandard Finite Difference Schemes for Differential Equations. *Journal of Difference Equations and Applications*. 2002; 8(9): 823-847.
- [26] Yuste SB. Weighted average finite difference methods for fractional diffusion equations. *Journal of Computational Physics*. 2006; 216(1): 264-274.
- [27] Zhu D, Kinoshita S, Cai D, Cole JB. Investigation of structural colors in *Morpho* butterflies using the nonstandard-finite-difference time-domain method: Effects of alternately stacked shelves and ridge density. *Physical Review E*. 2009; 80(5): 051924.
- [28] Moaddy K, Momani S, Hashim I. The non-standard finite difference scheme for linear fractional PDEs in fluid mechanics. *Computers and Mathematics with Applications*. 2011; 61(4): 1209-1216.
- [29] Mickens RE. *Applications of Nonstandard Finite Difference Schemes*. Singapore: World Scientific; 2000.
- [30] Yuste SB, Acedo L. An explicit finite difference method and a new von Neumann-type stability analysis for fractional diffusion equations. *SIAM Journal on Numerical Analysis*. 2005; 42(5): 1862-1874.
- [31] Ghafoor A, Fiaz M, Hussain M, Ullah A, Ismail E, Awwad F. Dynamics of the time-fractional reaction-diffusion coupled equations in biological and chemical processes. *Scientific Reports*. 2024; 14: 7549.
- [32] Lin Y, Xu C. Finite difference spectral approximations for the time-fractional diffusion equation. *Journal of Computational Physics*. 2007; 225(2): 1533-1552.



- [33] Li C, Zeng F, Liu F. Numerical solution of variable-order time-fractional diffusion equations with non-uniform meshes. *Applied Mathematics and Computation*. 2019; 356: 424-443.
- [34] Garrappa R. Numerical methods for fractional differential equations: A survey and a software tutorial. *Mathematics*. 2018; 6(2): 16.
- [35] Diethelm K. *The Analysis of Fractional Differential Equations: An Application-Oriented Exposition Using Differential Operators of Caputo Type*. Berlin: Springer Science & Business Media; 2010.